

# Slow escape decisions are swayed by trait anxiety

Bowen J. Fung<sup>1,4\*</sup>, Song Qi<sup>1,4</sup>, Demis Hassabis<sup>2</sup>, Nathaniel Daw<sup>3</sup> and Dean Mobbs<sup>1\*</sup>

**Theoretical models distinguish between neural responses elicited by distal threats and those evoked by more immediate threats<sup>1–3</sup>. Specifically, slower ‘cognitive’ fear responses towards distal threats involve a network of brain regions including the ventral hippocampus (vHPC) and medial prefrontal cortex (mPFC), while immediate ‘reactive’ fear responses rely on regions such as the periaqueductal grey<sup>4,5</sup>. However, it is unclear how anxiety and its neural substrates relate to these distinct defensive survival circuits. We tested whether individual differences in trait anxiety would impact escape behaviour and neural responses to slow and fast attacking predators: conditions designed to evoke cognitive and reactive fear, respectively. Behaviourally, we found that trait anxiety was not related to escape decisions for fast threats, but individuals with higher trait anxiety escaped earlier during slow threats. Functional magnetic resonance imaging showed that when subjects faced slow threats, trait anxiety positively correlated with activity in the vHPC, mPFC, amygdala and insula. Furthermore, the strength of functional coupling between two components of the cognitive circuit—the vHPC and mPFC—was correlated with the degree of trait anxiety. This suggests that anxiety predominantly affects cognitive fear circuits that are involved in volitional strategic escape.**

Anxiety is often described as an enduring, conscious state of apprehension. Theoretical work<sup>6–8</sup> proposes that anxiety is an emotional state independent of fear, which is instead evoked when a threat is increasingly proximal, and which ought to be minimally influenced by the anxiety state of the organism<sup>3,9</sup>. While this is generally well recognized in the non-human animal literature, researchers in the field of human affective neuroscience have paid relatively little attention to the question of whether anxiety and fear have different associated neural circuitry, and under what conditions anxiety might influence defensive behaviours in ecological scenarios. Moreover, recent advances have distinguished different classes of defensive responses that rely on distinct neural circuits, and which may complicate the theoretical relationship between fear and anxiety<sup>4,5</sup>.

Non-human animal research has shown that anxiety states involve a well-defined set of neural circuits<sup>10</sup>. The ventral hippocampus (vHPC) and medial prefrontal cortex (mPFC) are of particular interest as they have repeatedly been shown to be recruited during the regulation and representation of anxiety-provoking features of the environment<sup>11–14</sup>. The vHPC has input into the mPFC, and it appears to be the interaction between these regions that drives anxiety-related behaviours<sup>12</sup>. More recently, CA1 cells in the vHPC have been shown to exhibit stable representations of anxiety-provoking environments, and these cells drive avoidance behaviours<sup>15</sup>.

In humans, functional magnetic resonance imaging (fMRI) has been employed in conjunction with ‘active escape’ paradigms, the

goal of which is to evade an artificial predator with the capacity to chase, capture and shock the subject. Studies have shown that when an artificial predator is distant, increased activity is observed in the ventromedial prefrontal cortex (vmPFC)<sup>4</sup>. However, as the artificial predator moves closer, a switch to enhanced activation in the mid-brain periaqueductal grey (PAG) is observed<sup>4</sup>. More recently, our laboratory developed an escape decision task to demonstrate a similar ‘cognitive’ and ‘reactive’ fear differentiation of defensive survival circuits, by showing that fast escape decisions are associated with activity in the PAG<sup>5</sup> (a region shown previously to be involved in reactive flight<sup>4</sup>), while slower escape decisions rely on the vHPC, posterior cingulate cortex and mPFC<sup>5</sup> (a circuit implicated in behavioural flexibility and internal risk assessment<sup>16</sup>).

The vHPC–mPFC anxiety circuit therefore overlaps with the cognitive fear circuit recruited during these slower escape decisions<sup>3</sup>, but appears to be independent of reactive fear regions that are involved with threat under limited time constraints. In general, these reactive fear areas (for example, PAG) have limited interaction with higher-level cortical brain regions, thus are unlikely to be implicated in anxiety. Therefore, it is possible that while anxiety plays no role during imminent threat (when reactive fear circuits are recruited), it may be important within cognitive fear circuits, and subsequently affect defensive behaviour in the face of less imminent threats.

To provide evidence for this possibility, a critical question is whether individual differences in levels of trait anxiety selectively affect cognitive fear circuits during defensive decision-making, or whether reactive fear circuits are also influenced by the trait anxiety of the individual. Moreover, it is equally important to determine whether there are commensurate changes in survival behaviours and decision-making as a result of differences in trait anxiety, as would be expected if anxiety has an ethological origin<sup>6</sup>.

To address these questions, we reanalysed behavioural and neural data collected in our previously published study<sup>5</sup>, along with previously unanalysed trait anxiety data (the Spielberger State-Trait Anxiety Inventory Form Y (STAI-Y)<sup>17</sup>). In each trial of the behavioural task, participants passively earned money while they encountered virtual predators of three colours, each representing different attack distances (Fig. 1a). These attack distances were drawn from Gaussian distributions that were unique to the particular predator type. Fast attack predators (that is, early attacking) were characterized by the virtual predator quickly switching from slow approach to fast attack velocity, therefore requiring the subject to make quick escape decisions. In contrast, slow attack predators (that is, late attacking) slowly approached for longer time periods, resulting in larger buffer zones and more time to contemplate escape. It is important to emphasize that ‘fast’ and ‘slow’ here describe the timing of the predator attack, not the speed of the predators. The goal of the task was to try to successfully escape, while at the same time

<sup>1</sup>Division of the Humanities and Social Sciences, California Institute of Technology, Pasadena, CA, USA. <sup>2</sup>Google DeepMind, London, UK.

<sup>3</sup>Department of Psychology, Princeton University, Princeton, NJ, USA. <sup>4</sup>These authors contributed equally: Bowen J. Fung, Song Qi. \*e-mail: [bjfung@caltech.edu](mailto:bjfung@caltech.edu); [dmobbs@caltech.edu](mailto:dmobbs@caltech.edu)

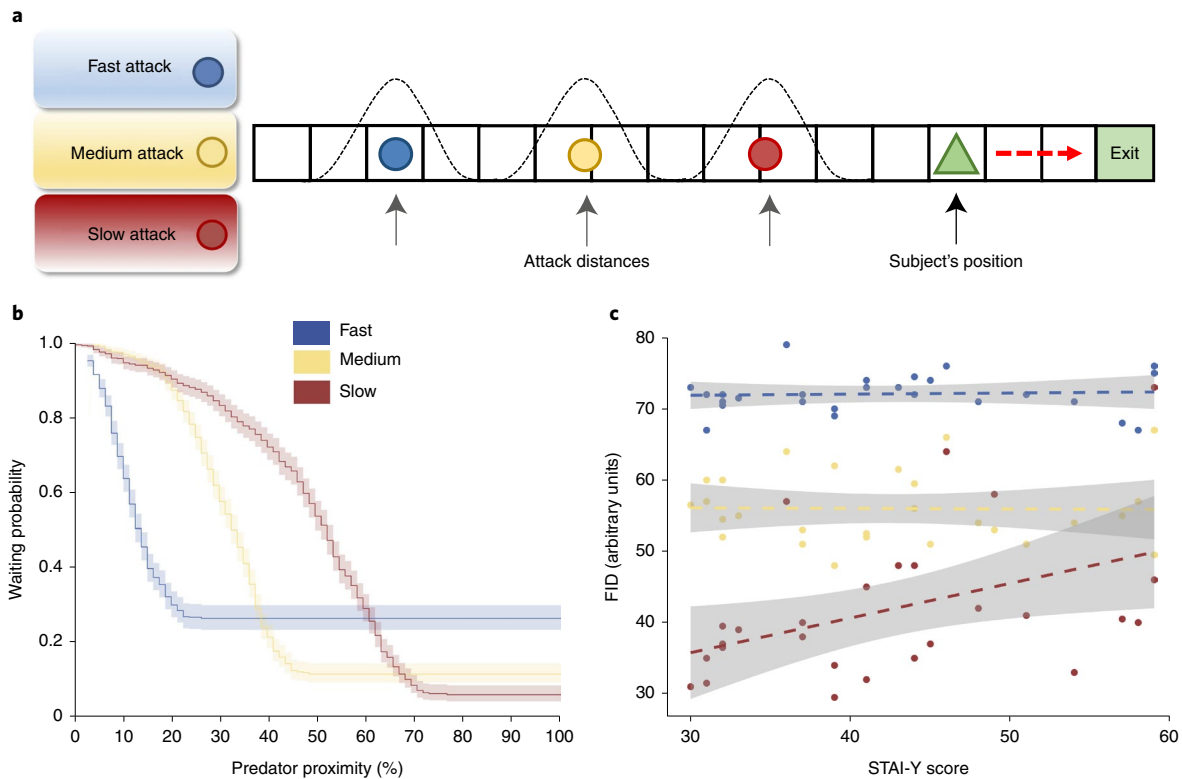


**Fig. 1 | FID experiment and behavioural results. a**, Predator escape setup. In each trial, participants were presented with a cue indicating the predator type. The predator would appear on the left side of the runway and slowly move towards the participant (green triangle). Participants passively accrued money while they waited, but at any time could press a button to begin their escape towards the exit. The predator would speed up (attack) at a random distance drawn from the respective Gaussian distributions shown above. If participants were caught by the predator, they would receive a mild electric shock and lose any money accrued on that trial. **b**, Kaplan-Meier survival curves for each predator type as a function of predator proximity. Curves reflect pooled data from all subjects ( $n=27$ ). Shaded areas represent 95% CIs. **c**, FID for each predator type as a function of STAI-Y score. Each dot corresponds to a single subject's median FID in one condition ( $n=27$ ). Dashed lines show the linear fit to the data. Shaded areas indicate s.e.

maximizing the amount of money earned by fleeing as late as possible (that is, at the shortest distance from the predator, or flight initiation distance (FID)).

Subjects performed this task while undergoing fMRI to assess the relative contributions of the 'reactive fear' and 'cognitive fear' networks to their escape decisions, and whether behaviour or brain activity in these circuits varied as a function of trait anxiety. Given the theoretical and neural differentiation between reactive fear and cognitive fear, we hypothesized that under conditions of slow predator attack, individuals with high trait anxiety would show preferential activity in the cognitive fear circuitry (relative to individuals with low trait anxiety), but no differences in the reactive fear circuitry. We also hypothesized that individuals scoring higher in trait anxiety would make earlier escape decisions, but only when there was sufficient time to assess the threat.

To test the hypothesis that trait anxiety would affect escape decisions, we estimated a mixed-effects linear regression model with subjects' median FIDs as the dependent variable and predator type and STAI-Y score as the independent variables (Table 1). Relative to the fast predator type, we observed the expected effects of the medium ( $t(2, 1,592.97)=-8.01$ ;  $P<0.001$ ; regression coefficient  $\beta=-17.88$ ; 95% confidence interval (CI) =  $-22.25$  to  $-13.51$ ) and slow ( $t(2, 1,592.97)=-23.12$ ;  $P<0.001$ ;  $\beta=-52.22$ ; 95% CI =  $-56.65$  to  $-47.79$ ) predator types. There was no significant main effect of STAI-Y score ( $t(1, 25.23)=0.09$ ;  $P=0.925$ ;  $\beta=0.01$ ; 95% CI =  $-0.21$  to  $0.19$ ), nor any significant interaction between STAI-Y score and the medium predator type ( $t(2, 1,593.32)=1.4$ ;  $P=0.908$ ;  $\beta=0.07$ ; 95% CI =  $-0.03$  to  $0.17$ ). However, we observed a significant

interaction effect between the slow predator type and STAI-Y score ( $t(2, 1,593.32)=10.94$ ;  $P<0.001$ ;  $\beta=0.57$ ; 95% CI =  $0.47$  to  $0.67$ ), suggesting that trait anxiety and FID were related, but only for the slow predator condition (see Fig. 1c).

It is important to note that participants had a larger time window in which to respond in the slow predator condition; therefore, the variance in escape distances was not equal across predator types. For details, as well as a control analysis taking into account the differences in variance, see the section 'Variability in flight initiation distance' in the Supplementary Information. Importantly, controlling for these variance differences resulted in no changes to our findings. We also collected data on the behavioural inhibition/activation scale. For an analysis of this scale, see the section 'Behavioural inhibition and flight initiation distance' in the Supplementary Information.

Note that because participants were given electrical stimulation when they were caught by the virtual predator, to obviate interference, it was necessary to exclude these trials from the imaging analysis reported below. For consistency, the behavioural analysis above also excluded unsuccessful escape trials. However, unsuccessful escape trials still contain information about subjects' tolerance to predator distance. To ensure that the analyses above were not biased by this possibility, we adopted a technique from survival analysis, which allowed us to take into account the unsuccessful trials as censored data. To appropriately prepare the data for this analysis (which is more commonly used to model time-based responses rather than distance-based responses), we transformed the dependent variable of FID by subtracting FID from the maximum FID,

**Table 1 | Activation table for second-level STAI-Y score correlation for the slow versus fast predator contrast**

Brain region	Left vs right	Cluster size	T score	MNI coordinates		
				x	y	z
Hippocampus	L	60	5.32	-15	-27	-6
Postcentral gyrus	L	209	4.91	-45	-18	54
mPFC	L	63	4.70	-3	51	-14
Insula	L	94	4.53	-40	8	-3
Insula	R	107	4.74	36	6	-6
Amygdala	R	15	4.93	22	0	-20

$P < 0.05$ , FDR corrected.

then normalizing this by the maximum FID. This new dependent variable can be thought of as predator proximity, expressed as a percentage. The Kaplan–Meier estimated survival curves (that is, the probability of waiting as a function of predator proximity) for each predator are shown in Fig. 1b.

To control for the potential effect of data censoring, we repeated the analysis of behavioural data using a mixed-effects Cox regression model on the probability of flight responses over time, which took into account predator type and participant heterogeneity. This model again revealed the expected effects of the medium ( $z = -3.34$ ;  $P < 0.001$ ;  $\beta = -0.98$ ; 95% CI =  $-1.55$  to  $-0.4$ ) and slow ( $z = -10.43$ ;  $P < 0.001$ ;  $\beta = -3.09$ ; 95% CI =  $-3.67$  to  $-2.51$ ) predator types. It also showed no significant main effect of STAI-Y score ( $z = -1.07$ ;  $P = 0.29$ ;  $\beta = -0.01$ ; 95% CI =  $-0.04$  to  $0.01$ ), nor a significant interaction between STAI-Y score and the medium predator type ( $z = 1.84$ ;  $P = 0.066$ ;  $\beta = 0.01$ ; 95% CI =  $< 0.01$  to  $0.03$ ). Importantly, it also again revealed a significant interaction effect between the slow predator type and STAI-Y score ( $z = 6.74$ ;  $P < 0.001$ ;  $\beta = 0.05$ ; 95% CI =  $0.03$  to  $0.6$ ). This effect had a hazard ratio of 1.05 (95% CI =  $1.03$  to  $1.06$ ), equivalent to a 5% increase in the chance of fleeing per unit increase of STAI-Y.

The results above provide clear evidence that trait anxiety influences subjects' propensity to escape earlier when given enough time to prepare an escape. However, it is unclear whether this should negatively affect their economic performance in the task. To test this, we performed a two-way repeated-measures analysis of variance (ANOVA), with predator type and STAI-Y score as independent variables and subjects' cumulative total earnings as the dependent variable. Given that subjects could earn more money in the slow predator condition, we first standardized reward scores for each predator type. There was no significant effect of predator type on standardized earnings ( $F(2, 52) = 0.34$ ;  $P = 0.667$ ; Greenhouse–Geisser correction factor,  $\epsilon = 0.81$ ; partial eta-squared effect size  $\eta_p^2 = 0.08$ ; 90% CI =  $0$  to  $0.07$ ), but we observed a significant main effect of STAI-Y score on total earnings ( $F(1, 26) = 4.32$ ;  $P = 0.048$ ;  $\eta_p^2 = 0.9$ ; 90% CI =  $< 0.01$  to  $0.34$ ), suggesting that subjects with higher STAI-Y scores had poorer economic performance in the task, across all predator types. There was no interaction effect of STAI-Y score and predator type ( $F(2, 52) = 0.36$ ;  $P = 0.656$ ;  $\epsilon = 0.81$ ;  $\eta_p^2 < 0.01$ ; 90% CI =  $0$  to  $0.07$ ).

Although economic gain is an index of performance in this task, it could be argued that the more ecologically important performance measure is escape success. Notably, subjects' economic performance and proportion of escape trials were not significantly correlated across all predator types ( $t(26) = 0.47$ ;  $P = 0.643$ ;  $r = 0.09$ ; 95% CI =  $-0.29$  to  $0.45$ ), nor within the slow predator condition ( $t(26) = -1.67$ ;  $P = 0.108$ ;  $r = -0.31$ ; 95% CI =  $-0.61$  to  $0.07$ ). To test whether trait anxiety was related to how frequently subjects successfully escaped the predators, we again performed a two-way repeated-measures ANOVA, with predator type and STAI-Y score

as independent variables and the proportion of successful escape trials as the dependent variable. While there were no main effects of STAI-Y score ( $F(1, 26) = 0.23$ ;  $P = 0.633$ ;  $\eta_p^2 < 0.01$ ; 90% CI =  $0$  to  $0.13$ ) or predator type ( $F(2, 52) = 1.89$ ;  $P = 0.175$ ;  $\epsilon = 0.53$ ;  $\eta_p^2 = 0.07$ ; 90% CI =  $0$  to  $0.17$ ), the ANOVA revealed a significant interaction effect between STAI-Y score and predator type ( $F(2, 52) = 4.46$ ;  $P = 0.031$ ;  $\epsilon = 0.68$ ;  $\eta_p^2 = 0.15$ ; 90% CI =  $0.02$  to  $0.27$ ). Simple effects analyses (one-way repeated-measures ANOVAs within each predator type) revealed a significant effect only for the slow predator type ( $F(1, 26) = 5.49$ ;  $P = 0.027$ ;  $\eta_p^2 = 0.17$ ; 90% CI =  $0.01$  to  $0.37$ ), but not for the fast ( $F(1, 26) = 2.12$ ;  $P = 0.158$ ;  $\eta_p^2 = 0.08$ ; 90% CI =  $0$  to  $0.26$ ) or medium predator ( $F(1, 26) = 0.39$ ;  $P = 0.536$ ;  $\eta_p^2 = 0.01$ ; 90% CI =  $0$  to  $0.15$ ). This suggested that, similar to the analysis of FID above, STAI-Y score was positively related to escape success in the slow predator condition, with no evidence for a relationship within the fast or medium predator condition. Overall, these results show that subjects with higher trait anxiety tended to more successfully escape predators, but that this also negatively impacted how much money they earned in the task (a summary of performance measures can be found in Supplementary Table 2).

Next, we tested our hypothesis that only during slow attack would we see a positive correlation between trait anxiety and activity in the cognitive fear circuitry. For this analysis, we excluded unsuccessful escape trials due to the interference of the electric stimulation on the blood-oxygen-level-dependent (BOLD) response (mean numbers of trials excluded were 6.88, 3.71 and 3.37, per subject, out of 23, 24 and 25, for the fast, medium and slow predator types, respectively). We focused on the 2 s before participants' flight initiation responses, which allowed us to examine the neural activity in anticipation of the escape response (detailed methodology of the base fMRI analysis can be found in ref. <sup>5</sup>). First, we contrasted the slow-attacking predator condition with the fast-attacking predator condition. Then, we used participants' STAI-Y scores as second-level regressors for this contrast, such that any significant increase in activity would indicate positive modulation by trait anxiety for the slow predator condition (for a similar analysis using contrasts for the slow and fast predators against a control condition, see Supplementary Information).

After thresholding and correction, we observed significant BOLD responses in regions including the amygdala, hippocampus, vmPFC and midcingulate cortex (Fig. 2a and Table 1). This was consistent with our hypothesis, and supported the behavioural findings whereby the STAI-Y score exclusively influences escape decisions when the threat is distant (in the case of the slow-attacking predator), but not when the threat is imminent (in the case of the fast-attacking predator). A visualization of BOLD response as a function of trait anxiety for select regions is shown in Supplementary Fig. 2.

To assess the interaction of brain regions involved in escape decisions, we performed a generalized psychophysiological interaction (gPPI) analysis<sup>18</sup>. Given the theoretical and empirically demonstrated involvement of the vHPC in cognitive fear and anxiety<sup>4,19</sup>, and because of its exhaustive bidirectional anatomical connections with the amygdala and its nuclei, as well as its functional role in fear, stress and emotion<sup>15,20,21</sup>, we chose vHPC as an independent seed region (see Supplementary Table 3 for a corresponding analysis using the entire hippocampus as a seed region). A corresponding structural region of interest was obtained using the WFU PickAtlas. This first-level gPPI analysis on the slow versus fast predator contrast is reported in ref. <sup>5</sup>, and will not be reported here for brevity. We then added STAI-Y score as a regressor in a second-level analysis. STAI-Y score significantly modulated the functional coupling between the vHPC seed, bilateral mPFC, right inferior frontal gyrus and left insula (Fig. 2b and Table 2). Overall, this suggests that these macrocircuits are those that facilitated the impact of STAI-Y score on escape decisions in the slow predator condition.

Our results provide evidence that trait anxiety can influence escape decisions, but only under conditions of relatively prolonged

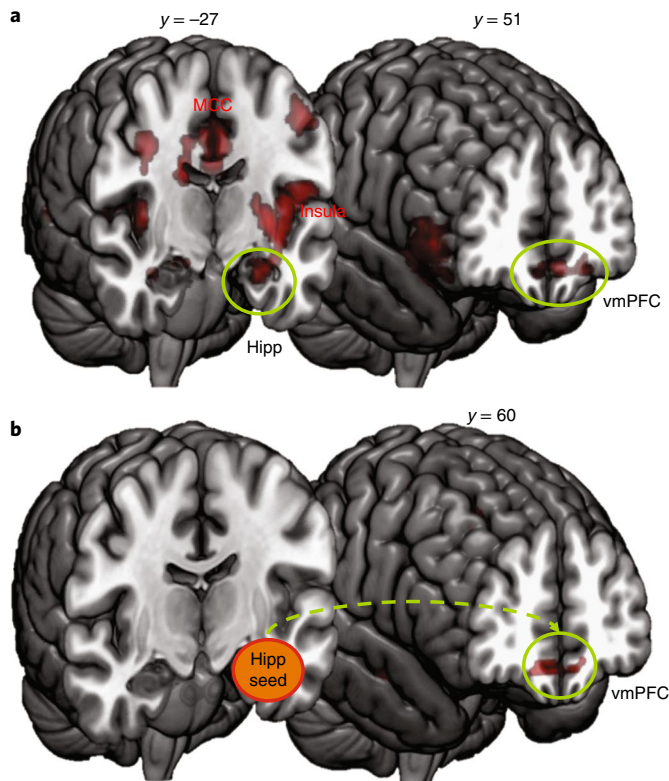


**Fig. 2 | Neural activity.** **a**, Neural activity associated with STAI-Y score for the slow versus fast predator contrast at two different coronal plane coordinates, given in Montreal Neurological Institute (MNI) space. Red areas represent significant activity thresholded at  $P < 0.05$  (false discovery rate (FDR) corrected). **b**, gPPI-coupled brain areas modulated by STAI-Y score. Hipp, hippocampus; MCC, mid cingulate cortex.

threat, compared with more imminent threats<sup>2,6,22</sup>. This disassociation implies that trait anxiety selectively affects decisions of different ethnological classes, as distinguished by the amount of time afforded for reflection and cognitive strategizing. The notion of dichotomous mapping between temporally proximal threats and fear, and temporally distal threats and anxiety is not new. For example, rodents' defensive behaviour differs when a threat is distal versus when it is immediate<sup>23</sup>, and anxiolytic drugs appear to only affect the former<sup>8</sup>. Likewise, previous models of threat evaluation have suggested that both anxious and non-anxious individuals will respond similarly to proximal threats, but individuals with high anxiety will exhibit differential behaviour in response to more distal threats<sup>1</sup>. Our study provides empirical evidence that trait anxiety selectively impacts escape decisions in humans under this specific class of threat.

The interpretation that trait anxiety affects only cognitive fear behaviour was supported by our neuroimaging results. These results showed that brain areas previously indicated to be involved with behavioural flexibility and information-processing aspects of fear responses (including the hippocampus, amygdala, mPFC and insula<sup>4,5,16</sup>) covaried with trait anxiety. However, areas associated with reactive fear—the PAG, superior colliculus, midcingulate cortex and central nucleus of the amygdala<sup>4,5,24</sup>—were not significantly affected by variability in anxiety. Notably, these findings strongly support theories based on defensive distance<sup>25</sup>, whereby defensive responses to immediate threats and dangers map onto low-level brain areas such as the PAG, whereas responses to physically or psychologically distal or anticipated threats map to higher-level areas such as the PFC<sup>24,26</sup>. Our findings extend these theories by providing a clear disassociation of the effects of trait anxiety on one circuit

over the other, with accompanying behavioural effects, in an ecologically relevant paradigm.

These seed-based functional coupling results are consistent with previous non-human animal studies showing functional interactions between the ventral and dorsal hippocampus and vmPFC in anxiety-provoking environments<sup>11,12,27</sup>. For example, local field potential recordings in rodents have shown that there is synchrony in theta oscillatory activity between vHPC and mPFC, and that this synchrony is increased in anxiogenic environments<sup>12</sup>. In addition, single-unit recordings have shown that cells in the mPFC have stronger anxiety-related firing patterns when phase-locked with local field potentials in the vHPC<sup>11</sup>. Using magnetoencephalography, others have corroborated these non-human animal findings in humans<sup>28</sup>. Our results parallel both the human and non-human animal evidence for functional coupling between the vHPC and mPFC, and further consolidate the characterization of this interaction with a different brain-imaging method.

The specific nature of the coupling between the vHPC and mPFC has garnered some previous discussion. For example, because vHPC–mPFC connections are unidirectional<sup>29</sup>, it has been suggested that the vHPC primes the mPFC to represent anxiety-related features of the environment, possibly using memories of threats to estimate threat probability<sup>28</sup>. The mPFC has efferent projections to the amygdala and PAG, and these connections have been suggested to be the downstream areas responsible for the initiation of defensive behavioural responses<sup>24,30</sup> and the inhibition of exploratory behaviours<sup>11</sup>. To complement this, the vHPC also has direct projections to the basolateral amygdala (BLA), bed nucleus of the stria terminalis and lateral hypothalamic area, which can also facilitate anxiety responses<sup>15</sup>.

In light of the results from our study, it is possible that vHPC may encode the previously learned threat context (that is, the predator condition) and relay this information to the mPFC where it influences strategic decision-making. Our results suggest that the observed increase in connectivity between the vHPC and mPFC in trait-anxious individuals may reflect a priming mechanism that lowered the threshold for escape responses, resulting in earlier escape decisions<sup>10</sup>. However, for the fast predator condition, this slow, deliberative priming is not sufficient; thus, the initiation of behavioural responses appears to bypass this connection. One compelling question is whether trait anxiety merely interacts with this vHPC–mPFC mechanism or whether it can be fully identified with information processing between these subregions. While we speculatively provide this neural mechanism for trait anxiety—which is also supported by the non-human animal literature—we emphasize that this requires causal corroboration, perhaps in the form of pharmaceutical manipulations in humans. While our study lacked the appropriate design and power for this approach, one further piece of evidence that would provide compelling support for such a mechanism would be trial-by-trial prediction of FID using brain activity in vHPC–mPFC.

Notably, we did not observe modulation of the BLA, bed nucleus of the stria terminalis or lateral hypothalamic area by trait anxiety. One likely possibility is that these areas are involved in longer-term anxiety responses, requiring the recruitment of corticotropin-releasing hormone<sup>23</sup>, and that our slow predator condition was not adequately protracted to cause these responses. Given that the BLA and amygdala have strong inputs to the vHPC<sup>31,32</sup>, another possibility is that these areas are more commonly recruited during fear learning (which we did not examine) and imbue the encoding of environmental stimuli with emotional salience (for example, ref. <sup>33</sup>). Indeed, most empirical evidence of the increased involvement of the amygdala in trait-anxious individuals has come from learning paradigms and studies of fear conditioning (for example, ref. <sup>34</sup>). Thus, trait anxiety is likely to affect both the encoding of threats and their retrieval from memory, potentially via different

**Table 2 | Activation table for second-level STAI-Y score correlation for gPPI (vHPC seed)**

Brain region	Left vs right	Cluster size	T score	MNI coordinates		
				x	y	z
Insula	L	49	5.13	-33	9	0
mPFC	R	168	5.00	15	60	-6
mPFC	L	124	5.18	-18	51	-6
Inferior frontal gyrus	R	38	5.11	42	15	9

$P < 0.05$ , FDR corrected.

neural substrates. This may be of critical importance for many clinical anxiety disorders (such as post-traumatic stress disorder) where threats have already been learned. One further possibility, as suggested previously<sup>28</sup>, is that the vHPC is specifically involved in threat memory retrieval only when there is approach–avoidance conflict<sup>35–37</sup>, as was the case with the trade-off between reward and threat of shock in our task.

Previous research has also suggested the possibility that mPFC representation of the environment depends on the strength of the vHPC input: moderate input appropriately signals the aversiveness of specific features, but strong input decreases discriminative capability, leading to generalized anxiety responses<sup>11</sup>. In our study, we were not able to evaluate individuals' abilities to discriminate between different levels of threat, but this would be a promising avenue for future research. In particular, this might suggest that populations with clinical anxiety disorders may exhibit increased coupling between the vHPC and mPFC across threat levels, and consequently faster escape decisions for all predator conditions.

The impact of trait anxiety on escape decisions could influence survival outcomes in at least two important ways<sup>38,39</sup>. First, if individuals with high trait anxiety escape predators earlier, they expedite other behaviours, such as foraging, and thus may accrue fewer primary rewards. Our results support this idea by showing that those with higher trait anxiety earned less total reward in our task. In contrast, it could be argued that a more survival-relevant performance metric is successful escape (additional reward is irrelevant if caught by a predator). Our results also showed that individuals with higher trait anxiety made a higher proportion of successful escape decisions. However, unlike reward, which was affected across all predator conditions, individuals with higher trait anxiety only made a higher proportion of successful escape decisions within the slow predator condition, in line with the idea that trait anxiety only affects flight decisions under these contexts. One possible explanation for this difference may have been that trait anxiety also affected escape responses in the medium and fast predator conditions, but to a lesser, non-significant degree. This is especially possible considering that there is some individual variability both in trait anxiety and performance in general; thus, our specification of cognitive and reactive fear classes will not have perfectly divided performance in these individuals. A series of experiments spanning a large range of predator conditions and reward contingencies may be able to address this issue with more clarity, and perhaps reveal population-level differences in how trait anxiety influences performance. Ultimately, both the accrual of reward and successful escape are important factors for survival, and differences in trait anxiety appear to arbitrate between these, depending on the threat context.

Coexisting with a disassociation of anxiety and fear based on defensive distance is a disassociation based on defensive direction<sup>26</sup>. The 'direction' of this construct refers to approach versus avoidance, and theoretical work proposes that fear drives avoidance of danger, while anxiety drives approach towards danger<sup>26</sup>. In our experimental

design, an approach–avoidance conflict existed between reward and the threat of shock. Because the slow predator condition allowed individuals to earn greater reward, this condition may have elicited greater relative anxiety. Under the defensive direction framework, we may have expected participants with higher trait anxiety to endure longer in this condition. However, we found that individuals scoring higher in trait anxiety escaped earlier, which speaks against defensive direction as a potential explanation for our behavioural results. However, it would be of interest for future experiments to more closely examine how defensive direction and trait anxiety relate to each other (see Supplementary Information for an analysis including a measure of behavioural inhibition).

Previous studies have also found evidence that anxiety can affect decision-making. For example, individuals with higher dispositional anxiety are more likely to be more risk averse in tasks such as the balloon analogue risk task<sup>40</sup>. Our study makes an important contribution to this literature by situating individuals in an ecological setting, where the effect of anxiety can be seen as a plausible adaptive role, rather than a straightforward deficit in decision-making. As such, our findings support evolutionary accounts of anxiety disorders<sup>41,42</sup>. While it is important to note that our current findings do not generalize to populations with clinical anxiety disorders, such as post-traumatic stress disorder, our hope is that future research will capitalize on the distinctions between threat contexts to better diagnose and treat these disorders. One potential avenue, for example, would be to tailor treatments and interventions based on individual differences in threat categorization.

Overall, this study provides strong empirical support for the notion that trait anxiety affects behaviour only when there is sufficient time to appropriately cognize a threat, and not when threats require an immediate reactive response. These behavioural results were borne out in an ecologically relevant paradigm, and were complemented with neural data that suggest that previously learned threat contexts more heavily influence strategic decision-making in trait-anxious individuals. The present study complements previous work describing the contexts under which reactive fear-defensive responses manifest<sup>3–5</sup>, and the behavioural and neural signatures of these responses, and in combination, they point to the importance of examining different ecological classes of threat in future work.

## Methods

A total of 30 subjects were recruited according to the guidelines of the Columbia University Institutional Review Board after providing informed consent. Data from one subject were lost due to a computer error. One additional subject was excluded due to excessive movement during the scan. Our final sample consisted of 28 subjects (17 female; age = 25.4 ± 7.3 years). No statistical methods were used to predetermine sample sizes, but our sample sizes were similar to those reported in previous publications<sup>4,5</sup>.

**Stimuli, apparatus and procedure.** This article constitutes an independent analysis of data from a previously published study<sup>3</sup>, with detailed methods reported here for completeness. Participants completed a computer-based task while in an fMRI scanner. The goal of the task was to earn as much money as possible while avoiding being caught by a virtual predator. Before the beginning of each trial, participants were presented with a 2 s cue indicating one of three different predator types that would be present in the upcoming trial. The participants were then shown a two-dimensional runway (distance: 90 units) with a triangle icon representing the position of the participant towards the right of the runway (at a distance of 80 units) and a circle icon representing the position of a predator at the left side of the runway (at a distance of 1 unit). This predator had two distinct modes of movement. In 'approach' mode, the predator would proceed rightwards along the runway at 4 units s<sup>-1</sup>. At a randomly chosen distance (that is, the attack distance), the predator would switch to 'chase' mode, at which point it would advance at 10 units s<sup>-1</sup>. These attack distances were randomly sampled from one of three Gaussian distributions, with means of 25, 40 and 50 (s.d.: 20, 20 and 20) for the slow, medium and fast predator types, respectively. Note that these predator types differed only in their mean attack distance, and not in the speed of their attack. Participants would passively gain money at a rate of 2 cents s<sup>-1</sup> while they remained on the runway, and at any time could press a button to begin an escape towards the

right side of the runway at 2 units  $s^{-1}$ . Notably, if participants did not respond before the predator reached its attack distance, it was not possible for them to escape. This prevented participants from merely relying on their reaction time by responding after the predator switched modes. If participants escaped successfully, they would earn the monetary reward accumulated during that trial. If they failed to escape successfully (that is, were caught by the predator) participants were given a mildly aversive electric shock (the shock magnitude was calibrated to each individual before testing), and the monetary reward earned in that trial was forfeit. Thus, to perform this task optimally, participants had to learn the distributions of attack distances for each of the predator types and respond as late as possible, provided the distance between them and the predator (that is, the FID) was sufficient for a successful escape. Before the beginning of this main task, participants completed a brief, eight-trial practice session to familiarize themselves with the paradigm. The attack distances of the predators were drawn from different distributions from those used in the main task. Participants then completed 96 trials of the main task. After 48 trials, the predator-colour cue was reassigned to maintain the attentional demands of the task. Participants also performed a matching control condition for each predator type, without the risk of shock or the incentive of monetary reward, but otherwise identical to the main task. After completion of the computer task, subjects were asked to complete a series of personality questionnaires that included the trait subscale of the STAI-Y<sup>17</sup> and the behavioural inhibition system/behavioural activation system scale<sup>43</sup> (see Supplementary Fig. 1 and Supplementary Methods for an analysis of behavioural inhibition system scores). The computer task was programmed in Cogent with MATLAB. Data collection and analysis were not performed blind to the conditions of the experiments.

All fMRI data were acquired using a GE Discovery MR750 3.0T scanner with 32-channel head coil. The imaging session consisted of two function scans (each 20 min), as well as a high-resolution anatomical T1-weighted image (1 mm isotropic resolution) collected at the beginning of each scan session. For functional imaging, interleaved T2\*-weighted gradient-echo echo-planar imaging sequences were used to produce 45 3-mm-thick oblique axial slices (repetition time = 2 s; echo time = 25 ms; flip angle = 77; field of view = 192 mm × 192 mm; matrix = 64 × 64). Each functional run began with 5 volumes (1,000 ms) before the first stimulus onset. These volumes were discarded before entering the analysis to allow for magnetic field equilibration. Participants viewed the screen via a mirror mounted on the head coil, and a pillow and foam cushions were placed inside the coil to minimize head movement. Electric stimulation was delivered using a BIOPAC STM100C.

**Data analysis.** All statistical analyses for the behavioural data were carried out in R<sup>44</sup> using the packages ezANOVA<sup>45</sup>, coxme<sup>46</sup> and lme4 (ref. 47) (see Supplementary Software). Before analyses, data were tested for normality and equal variances using Shapiro–Wilk and Mauchly's sphericity tests, respectively. Where appropriate, log transformations of the data were performed to account for non-normality and Greenhouse–Geisser corrections were performed to account for violations of sphericity, with  $\epsilon$  values and original degrees of freedom reported. For mixed models,  $P$  values were generated from Satterthwaite approximations to degrees of freedom. Confidence intervals are 90% for eta-squared effect sizes and 95% for all other effect sizes. Where appropriate, we corrected for multiple comparisons using the Holm–Bonferroni method. All tests were two tailed unless otherwise specified. We used an alpha level of 0.05 for all statistical tests.

Analysis of fMRI data was carried out using scripted batches in SPM8 software (Wellcome Trust Centre for Neuroimaging) implemented in MATLAB 7 (MathWorks). Structural images were subjected to the unified segmentation algorithm implemented in SPM8, yielding discrete cosine transform spatial warping coefficients used to normalize each individual's data into Montreal Neurological Institute (MNI) space. Functional data were first corrected for slice timing difference, and subsequently realigned to account for head movements. Normalized data were finally smoothed with a 6 mm full-width at half-maximum Gaussian kernel.

Preprocessed images were subjected to a two-level general linear model using SPM8. The first level contained the following regressors of interest, each convolved with the canonical two-gamma haemodynamic response function: a 2 s boxcar function for the onset of the trial (during predator-type cue presentation); a 4–8 s (duration-jittered) boxcar function from the onset to 2 s before participants' flight decisions; a 2 s boxcar function for the time before participants' flight decisions; and a 4–8 s (duration-jittered) boxcar function for the remainder of the trial. Mean-centred STAI-Y score ratings were included as orthogonal regressors. In addition, nuisance regressors consisted of motion parameters determined during preprocessing, their first temporal derivative and discrete cosine transform-based temporal low-frequency drift regressors with a cutoff of 192 s. Beta maps were used to create linear contrast maps, which were then subjected to second-level, random-effects one-sample  $t$ -tests. In addition, a flexible factorial model was used to examine the main effects of predator type. The resulting statistical maps were thresholded at  $P < 0.05$ , and we corrected for multiple comparisons using false discovery rate (FDR) correction (FDR whole-brain corrected)<sup>48,49</sup>.

After whole-brain analyses, a hypothesis-driven region of interest analysis was performed. These regions were chosen based on the results from a previous study using the same behavioural task (see ref. 5).

The functional connectivity analysis was performed for the response phase (escape decision) using a gPPI approach<sup>18</sup>. The vHPC was chosen as the seed region for subsequent gPPI analysis due to its functional role in fear, stress and emotion<sup>4,9</sup> and its empirically demonstrated involvement in our previous study<sup>5</sup>. See Supplementary Information for a similar analysis that includes the dorsal hippocampus. In the gPPI model, regressors of interest included the three predator conditions (slow, medium and fast), their corresponding control conditions and the gPPI terms for the above-mentioned six conditions. Using the gPPI toolbox<sup>18</sup>, a first-level connectivity analysis was carried out based on the gPPI term of the direct comparison between the two predator conditions (slow versus fast attacking predator). A similar connectivity analysis based on the gPPI term of the comparison between the slow predator and control condition can be found in the Supplementary Information. As a second-level analysis, STAI-Y score was then introduced as a covariate to examine how trait anxiety alters the strength of the gPPI with respect to the seed regions.

**Reporting Summary.** Further information on research design is available in the Nature Research Reporting Summary linked to this article.

### Data availability

Behavioural data can be found on the Open Science Framework (<https://osf.io/c4qbr/>). fMRI data are available from the corresponding author on reasonable request.

### Code availability

Code for all behavioural analyses can be found on the Open Science Framework (<https://osf.io/c4qbr/>). fMRI analysis code is available from the corresponding author on reasonable request.

Received: 29 May 2018; Accepted: 25 March 2019;

Published online: 20 May 2019

### References

- Mathews, A. & Mackintosh, B. A cognitive model of selective processing in anxiety. *Cogn. Ther. Res.* **22**, 539–560 (1998).
- Mobbs, D., Hagan, C. C., Dalgleish, T., Silston, B. & Prevoost, C. The ecology of human fear: survival optimization and the nervous system. *Front. Neurosci.* **9**, 55 (2015).
- Mobbs, D. The ethological deconstruction of fear(s). *Curr. Opin. Behav. Sci.* **24**, 32–37 (2018).
- Mobbs, D. et al. When fear is near: threat imminence elicits prefrontal-periaqueductal gray shifts in humans. *Science* **317**, 1079–1083 (2007).
- Qi, S. et al. How cognitive and reactive fear circuits optimize escape decisions in humans. *Proc. Natl Acad. Sci. USA* **115**, 3186–3191 (2018).
- Mobbs, D. & Kim, J. J. Neuroethological studies of fear, anxiety, and risky decision-making in rodents and humans. *Curr. Opin. Behav. Sci.* **5**, 8–15 (2015).
- LeDoux, J. Rethinking the emotional brain. *Neuron* **73**, 653–676 (2012).
- Blanchard, R. J., Yudko, E. B., Rodgers, R. J. & Blanchard, D. C. Defense system psychopharmacology: an ethological approach to the pharmacology of fear and anxiety. *Behav. Brain Res.* **58**, 155–165 (1993).
- Fanselow, M. S. & Lester, L. S. in *Evolution and Learning* (eds Bolles, R. C. & Beecher, M.) 185–211 (Lawrence Erlbaum Associates, 1988).
- Calhoun, G. G. & Tye, K. M. Resolving the neural circuits of anxiety. *Nat. Neurosci.* **18**, 1394–1404 (2015).
- Adhikari, A., Topiwala, M. A. & Gordon, J. A. Single units in the medial prefrontal cortex with anxiety-related firing patterns are preferentially influenced by ventral hippocampal activity. *Neuron* **71**, 898–910 (2011).
- Adhikari, A., Topiwala, M. A. & Gordon, J. A. Synchronized activity between the ventral hippocampus and the medial prefrontal cortex during anxiety. *Neuron* **65**, 257–269 (2010).
- Padilla-Coreano, N. et al. Direct ventral hippocampal-prefrontal input is required for anxiety-related neural activity and behavior. *Neuron* **89**, 857–866 (2016).
- Benoit, R. G., Davies, D. J. & Anderson, M. C. Reducing future fears by suppressing the brain mechanisms underlying episodic simulation. *Proc. Natl Acad. Sci. USA* **113**, E8492–E8501 (2016).
- Jimenez, J. C. et al. Anxiety cells in a hippocampal-hypothalamic circuit. *Neuron* **97**, 670–683.e6 (2018).
- McNaughton, N. & Corr, P. J. Survival circuits and risk assessment. *Curr. Opin. Behav. Sci.* **24**, 14–20 (2018).
- Spielberger, C., Gorsuch, R., Lushene, R., Vagg, P. & Jacobs, G. *Manual for the State-Trait Anxiety Inventory* (Consulting Psychologists Press, 1983).
- McLaren, D. G., Ries, M. L., Xu, G. & Johnson, S. C. A generalized form of context-dependent psychophysiological interactions (gPPI): a comparison to standard approaches. *NeuroImage* **61**, 1277–1286 (2012).

19. McHugh, S., Deacon, R., Rawlins, J. & Bannerman, D. M. Amygdala and ventral hippocampus contribute differentially to mechanisms of fear and anxiety. *Behav. Neurosci.* **118**, 63–78 (2004).
20. Fanselow, M. S. & Dong, H.-W. Are the dorsal and ventral hippocampus functionally distinct structures? *Neuron* **65**, 7–19 (2010).
21. Moser, M.-B. & Moser, E. I. Functional differentiation in the hippocampus. *Hippocampus* **8**, 608–619 (1998).
22. Lima, S. L. & Dill, L. M. Behavioral decisions made under the risk of predation: a review and prospectus. *Can. J. Zool.* **68**, 619–640 (1990).
23. Davis, M., Walker, D. L., Miles, L. & Grillon, C. Phasic vs sustained fear in rats and humans: role of the extended amygdala in fear vs anxiety. *Neuropsychopharmacology* **35**, 105–135 (2010).
24. Graeff, F. G. Neuroanatomy and neurotransmitter regulation of defensive behaviors and related emotions in mammals. *Braz. J. Med. Biol. Res.* **27**, 811–829 (1994).
25. Blanchard, R. J. & Blanchard, D. C. An experimental analysis of defense, fear, and anxiety. In *Otago Conference Series No. 1. Anxiety* (eds McNaughton, N. & Andrews, G.) 124–133 (Univ. Otago Press, 1990).
26. McNaughton, N. & Corr, P. J. A two-dimensional neuropsychology of defense: fear/anxiety and defensive distance. *Neurosci. Biobehav. Rev.* **28**, 285–305 (2004).
27. Young, C. K. & McNaughton, N. Coupling of theta oscillations between anterior and posterior midline cortex and with the hippocampus in freely behaving rats. *Cereb. Cortex* **19**, 24–40 (2008).
28. Khemka, S., Barnes, G., Dolan, R. J. & Bach, D. R. Dissecting the function of hippocampal oscillations in a human anxiety model. *J. Neurosci.* **37**, 6869–6876 (2017).
29. Parent, M. A., Wang, L., Su, J., Netoff, T. & Yuan, L.-L. Identification of the hippocampal input to medial prefrontal cortex in vitro. *Cereb. Cortex* **20**, 393–403 (2009).
30. Vertes, R. P. Differential projections of the infralimbic and prelimbic cortex in the rat. *Synapse* **51**, 32–58 (2004).
31. Felix-Ortiz, A. C. et al. BLA to vHPC inputs modulate anxiety-related behaviors. *Neuron* **79**, 658–664 (2013).
32. Felix-Ortiz, A. C. & Tye, K. M. Amygdala inputs to the ventral hippocampus bidirectionally modulate social behavior. *J. Neurosci.* **34**, 586–595 (2014).
33. Malvaez, M. et al. Basolateral amygdala rapid glutamate release encodes an outcome-specific representation vital for reward-predictive cues to selectively invigorate reward-seeking actions. *Sci. Rep.* **5**, 12511 (2015).
34. Indovina, I., Robbins, T. W., Núñez-Elizalde, A. O., Dunn, B. D. & Bishop, S. J. Fear-conditioning mechanisms associated with trait vulnerability to anxiety in humans. *Neuron* **69**, 563–571 (2011).
35. Bach, D. R. et al. Human hippocampus arbitrates approach–avoidance conflict. *Curr. Biol.* **24**, 541–547 (2014).
36. Ito, R. & Lee, A. C. The role of the hippocampus in approach–avoidance conflict decision-making: evidence from rodent and human studies. *Behav. Brain Res.* **313**, 345–357 (2016).
37. Oehrn, C. R. et al. Human hippocampal dynamics during response conflict. *Curr. Biol.* **25**, 2307–2313 (2015).
38. Mathews, A. Why worry? The cognitive function of anxiety. *Behav. Res. Ther.* **28**, 455–468 (1990).
39. Perkins, A. M. & Corr, P. J. in *The Positive Side of Negative Emotions* (ed. Parrott, G.) 37 (Guilford Press, 2014).
40. Maner, J. K. et al. Dispositional anxiety and risk-avoidant decision-making. *Pers. Individ. Differ.* **42**, 665–675 (2007).
41. Meacham, F. & T. Bergstrom, C. Adaptive behavior can produce maladaptive anxiety due to individual differences in experience. *Evol. Med. Public Health* **2016**, 270–285 (2016).
42. Marks, I. & Nesse, R. M. Fear and fitness: an evolutionary analysis of anxiety disorders. *Ethol. Sociobiol.* **15**, 247–261 (1994).
43. Carver, C. S. & White, T. L. Behavioral inhibition, behavioral activation, and affective responses to impending reward and punishment: the BIS/BAS scales. *J. Pers. Soc. Psychol.* **67**, 319–333 (1994).
44. R Development Core Team R: *A Language and Environment for Statistical Computing* (R Foundation for Statistical Computing, 2013).
45. Lawrence, M. A. ez: Easy analysis and visualization of factorial experiments. R package version 4.4-0 (2016).
46. Therneau, T. M. coxme: Mixed effects cox models. R package version 2.2-5 (2015).
47. Bates, D., Machler, M., Bolker, B. & Walker, S. Fitting linear mixed-effects models using lme4. *J. Stat. Softw.* **67**, 1–48 (2015).
48. Genovese, C. R., Lazar, N. A. & Nichols, T. Thresholding of statistical maps in functional neuroimaging using the false discovery rate. *NeuroImage* **15**, 870–878 (2002).
49. Gray, J. A. The psychophysiological basis of introversion–extraversion. *Behav. Res. Ther.* **8**, 249–266 (1970).

### Acknowledgements

This work was supported by the National Institute of Mental Health (grant 2P50MH094258 to D.M.) and funds from the Tianqiao and Chrissy Chen Institute (P2026052 to D.M.). The funders had no role in study design, data collection and analysis, decision to publish or preparation of the manuscript.

### Author contributions

S.Q., D.H., N.D. and D.M. contributed to the conception and design of the experiment. S.Q. conducted the experiment and collected the data. S.Q. and B.J.F. analysed the data. B.J.F., S.Q. and D.M. drafted the manuscript. All authors reviewed the manuscript and gave final approval for publication.

### Competing interests

The authors declare no competing interests.

### Additional information

**Supplementary information** is available for this paper at <https://doi.org/10.1038/s41562-019-0595-5>.

**Reprints and permissions information** is available at [www.nature.com/reprints](http://www.nature.com/reprints).

**Correspondence and requests for materials** should be addressed to B.J.F. or D.M.

**Publisher's note:** Springer Nature remains neutral with regard to jurisdictional claims in published maps and institutional affiliations.

© The Author(s), under exclusive licence to Springer Nature Limited 2019

## Reporting Summary

Nature Research wishes to improve the reproducibility of the work that we publish. This form provides structure for consistency and transparency in reporting. For further information on Nature Research policies, see [Authors & Referees](#) and the [Editorial Policy Checklist](#).

### Statistics

For all statistical analyses, confirm that the following items are present in the figure legend, table legend, main text, or Methods section.

n/a Confirmed

- The exact sample size ( $n$ ) for each experimental group/condition, given as a discrete number and unit of measurement
- A statement on whether measurements were taken from distinct samples or whether the same sample was measured repeatedly
- The statistical test(s) used AND whether they are one- or two-sided  
*Only common tests should be described solely by name; describe more complex techniques in the Methods section.*
- A description of all covariates tested
- A description of any assumptions or corrections, such as tests of normality and adjustment for multiple comparisons
- A full description of the statistical parameters including central tendency (e.g. means) or other basic estimates (e.g. regression coefficient) AND variation (e.g. standard deviation) or associated estimates of uncertainty (e.g. confidence intervals)
- For null hypothesis testing, the test statistic (e.g.  $F$ ,  $t$ ,  $r$ ) with confidence intervals, effect sizes, degrees of freedom and  $P$  value noted  
*Give  $P$  values as exact values whenever suitable.*
- For Bayesian analysis, information on the choice of priors and Markov chain Monte Carlo settings
- For hierarchical and complex designs, identification of the appropriate level for tests and full reporting of outcomes
- Estimates of effect sizes (e.g. Cohen's  $d$ , Pearson's  $r$ ), indicating how they were calculated

*Our web collection on [statistics for biologists](#) contains articles on many of the points above.*

### Software and code

Policy information about [availability of computer code](#)

Data collection

Data analysis

For manuscripts utilizing custom algorithms or software that are central to the research but not yet described in published literature, software must be made available to editors/reviewers. We strongly encourage code deposition in a community repository (e.g. GitHub). See the Nature Research [guidelines for submitting code & software](#) for further information.

### Data

Policy information about [availability of data](#)

All manuscripts must include a [data availability statement](#). This statement should provide the following information, where applicable:

- Accession codes, unique identifiers, or web links for publicly available datasets
- A list of figures that have associated raw data
- A description of any restrictions on data availability

Behavioral data and accompanying code for all behavioral analyses and figures can be found on the Open Science Framework (<https://osf.io/c4qbr/>). fMRI data and analysis code are available from the corresponding author on reasonable request.

## Field-specific reporting

Please select the one below that is the best fit for your research. If you are not sure, read the appropriate sections before making your selection.

- Life sciences  Behavioural & social sciences  Ecological, evolutionary & environmental sciences

## Behavioural & social sciences study design

All studies must disclose on these points even when the disclosure is negative.

Study description	This study constitutes a quantitative experimental design.
Research sample	The participant sample consistent primarily of students recruited from Columbia University.
Sampling strategy	We employed a convenience sampling approach.
Data collection	A computer was used to collect behavioral data. Electric stimulation was delivered using a BIOPAC STM100C. All fMRI data were acquired using a GE Discovery MR750 3.0 T scanner with 32-channel headcoil.
Timing	<i>Indicate the start and stop dates of data collection. If there is a gap between collection periods, state the dates for each sample cohort.</i>
Data exclusions	Data from one subject was lost due to computer error. One additional subject was excluded due to excessive movement during the scan (this was an established exclusion criteria). Our final sample consisted of 28 subjects.
Non-participation	No participants declined participation.
Randomization	This was a repeated measures design. Conditions were counterbalanced.

## Reporting for specific materials, systems and methods

We require information from authors about some types of materials, experimental systems and methods used in many studies. Here, indicate whether each material, system or method listed is relevant to your study. If you are not sure if a list item applies to your research, read the appropriate section before selecting a response.

### Materials & experimental systems

n/a	Included in the study
<input checked="" type="checkbox"/>	<input type="checkbox"/> Antibodies
<input checked="" type="checkbox"/>	<input type="checkbox"/> Eukaryotic cell lines
<input checked="" type="checkbox"/>	<input type="checkbox"/> Palaeontology
<input checked="" type="checkbox"/>	<input type="checkbox"/> Animals and other organisms
<input type="checkbox"/>	<input checked="" type="checkbox"/> Human research participants
<input checked="" type="checkbox"/>	<input type="checkbox"/> Clinical data

### Methods

n/a	Included in the study
<input checked="" type="checkbox"/>	<input type="checkbox"/> ChIP-seq
<input checked="" type="checkbox"/>	<input type="checkbox"/> Flow cytometry
<input type="checkbox"/>	<input checked="" type="checkbox"/> MRI-based neuroimaging

## Human research participants

Policy information about [studies involving human research participants](#)

Population characteristics	Participants were healthy, right-handed. 17 of 28 were female. Mean age was 25.4 +- 7.3 years.
Recruitment	Participants were recruited according to the guidelines of the Columbia University Institutional Review Board after providing informed consent.
Ethics oversight	Columbia University Institutional Review Board.

Note that full information on the approval of the study protocol must also be provided in the manuscript.

## Magnetic resonance imaging

### Experimental design

Design type	Task-based, event related design.
Design specifications	There were 96 trials per subject, each 11.75 seconds average in duration.
Behavioral performance measures	A single response was measured from subjects on each trial; the distance at which they made a response.

## Acquisition

Imaging type(s)	Functional and anatomical.
Field strength	3.0T
Sequence & imaging parameters	For functional imaging, interleaved T2*-weighted gradient-echo echo planar imaging (EPI) sequences were used to produce 45 3-mm-thick oblique axial slices (TR = 2 s., TE = 25 ms, flip angle = 77, FOV = 192 x 192 mm, matrix = 64 x 64)
Area of acquisition	Whole brain.
Diffusion MRI	<input type="checkbox"/> Used <input checked="" type="checkbox"/> Not used

## Preprocessing

Preprocessing software	SPM8 software (Wellcome Trust Centre for Neuroimaging, London, UK) implemented in Matlab 7 (The MathWorks Inc., Natick MA). Structural images were subjected to the unified segmentation algorithm implemented in SPM8, yielding discrete cosine transform spatial warping coefficients used to normalize each individual's data into MNI space. Functional data were first corrected for slice timing difference, and subsequently realigned to account for head movements. Normalized data were finally smoothed with a 6-mm FWHM Gaussian kernel.
Normalization	See above.
Normalization template	See above.
Noise and artifact removal	See above.
Volume censoring	No volumes were censored.

## Statistical modeling & inference

Model type and settings	Preprocessed images were subjected to a two-level general linear model using SPM8. The first level contained the following regressors of interest, each convolved with the canonical two-gamma hemodynamic response function: a 2 s box-car function for the onset of the trial (during predator type cue presentation), a 4-8 s (duration jittered) box-car function from the onset to 2 s prior to participants' flight decisions, a 2 s boxcar function for the time prior to participants' flight decisions, and a 4-8 s (duration jittered) box-car function for the remainder of the trial. Mean-centered trait anxiety ratings were included as orthogonal regressors. In addition, nuisance regressors consisted of motion parameters determined during preprocessing, their first temporal derivative and discrete cosine transform-based temporal low frequency drift regressors with a cutoff of 192 s. Beta maps were used to create linear contrast maps, which were then subjected to second-level, random-effects one-sample t tests. In addition, A flexible factorial model was used to examine the main effects of predator type. The resulting statistical maps were thresholded at $p < 0.05$ , and we corrected for multiple comparisons using false discovery rate correction (FDR whole brain corrected). The functional connectivity analysis was performed for the response phase (escape decision) using a generalized psychophysiological interactions (PPI) approach.
Effect(s) tested	We tested contrasts between predator conditions and their modulation by trait anxiety.
Specify type of analysis:	<input type="checkbox"/> Whole brain <input type="checkbox"/> ROI-based <input checked="" type="checkbox"/> Both
Anatomical location(s)	We determined vHPC as an independent seed region given background literature. The corresponding structural ROI was obtained using the WFU Pickatalas.
Statistic type for inference (See <a href="#">Eklund et al. 2016</a> )	Voxel-wise, see above.
Correction	See above.

## Models & analysis

n/a	Involved in the study
<input checked="" type="checkbox"/>	<input type="checkbox"/> Functional and/or effective connectivity
<input checked="" type="checkbox"/>	<input type="checkbox"/> Graph analysis
<input checked="" type="checkbox"/>	<input type="checkbox"/> Multivariate modeling or predictive analysis